

Water-soluble inhibitor on microbiologically influenced corrosion in diesel pipeline

N. Muthukumar, S. Maruthamuthu, N. Palaniswamy*

Corrosion Protection Division, Central Electrochemical Research Institute, Karaikudi 630 006, India

Received 6 July 2006; received in revised form 5 September 2006; accepted 26 September 2006

Available online 7 October 2006

Abstract

The effect of water-soluble corrosion inhibitor on the growth of bacteria and its corrosion inhibition efficiency were investigated. Corrosion inhibition efficiency was studied by rotating cage test and flow loop techniques. The nature of biodegradation of corrosion inhibitor was also analyzed by using Fourier transform infrared spectroscopy (FT-IR), nuclear magnetic resonance spectroscopy (NMR) and Gas chromatography and mass spectrometer (GC-MS). The bacterial isolates (*Serratia marcescens* ACE2, *Bacillus cereus* ACE4) have the capacity to degrade the aromatic and aliphatic hydrocarbon present in the corrosion inhibitor. The degraded products of corrosion inhibitor and bacterial activity determine the electrochemical behaviour of API 5LX steel. The influence of bacterial activity on degradation of corrosion inhibitor and its influence on corrosion of API 5LX have been evaluated by employing weight loss techniques and electrochemical studies. The main finding of this paper is that the water-soluble corrosion inhibitor is consumed by the microbial action, which contributes to the decrease in inhibitor efficiency. The present study also emphasizes the importance of evaluation of water-soluble corrosion inhibitor in stagnant model (flow loop test) and discusses the demerits of the water-soluble corrosion inhibitors in petroleum product pipeline.

© 2006 Elsevier B.V. All rights reserved.

Keywords: Diesel pipeline; Water-soluble corrosion inhibitor; Rotating cage; Flow loop method; Biodegradation; Microbiologically influenced corrosion

1. Introduction

The possible effect of corrosion inhibitor on bacteria is of considerable interest to people involved in oil and gas production and transmission pipelines. It is possible that corrosion inhibitors will have biocidal effects on bacteria [1]. Organic film-forming inhibitors used in the oil and gas industry are generally of the cationic/anionic type and include imidazolines, primary amines, diamines, amino-amines, oxyalkylated amines, fatty acids, dimmer-trimer acids, naphtheneic acid, phosphate esters and dodecyl benzene sulphonic acids. Their mechanism of action is to form a persistent monolayer film adsorbed at the metal/solution interface. It is well known that bacteria can oxidize a wide variety of chemicals and use them as nutrient source and enhance the proliferation of bacteria [2–4]. However aerobic bacteria and fungi participate in the corrosion process [5–7]. The microorganisms influence the corrosion by altering

the chemistry at the interface between the metal and the bulk fluid [8,9]. Thus, the alteration of the molecule of the inhibitor caused by microbial degradation during their use, can affect their specific performance on corrosion inhibition [10]. Microbial degradation of simple heterocyclic inhibitor of the type morpholine (C_4H_9NO) has been recently reported by Poupin et al. [11]. Bento et al. [12] and Muthukumar et al. [13] have reported that the understanding of the microbial species involved in microbial corrosion and their interactions with metal surfaces. The degradation involved an enzymatic attack at the C–N position, followed by ring cleavage to produce glycolic acid [11]. Dominguez et al. [14] (1998) reported the loss in efficiency of organic corrosion inhibitors in the presence of *Pseudomonas fluorescens* isolated from injection water system used in off-shore oil production.

Recently Maruthamuthu et al. [15] and Rajasekar et al. [4] have noticed the degradation of corrosion inhibitors and their effect on the corrosion process in a petroleum product transporting pipeline at northwest, India. In petroleum product pipelines, it would be better to know if the water-soluble corrosion inhibitor is acting as a nutrient source or as biocide or indeed whether what

* Corresponding author. Tel.: +91 4565 227550; fax: +91 4565 227779.
E-mail address: swamy23@rediffmail.com (N. Palaniswamy).

its effect at all. In the present study, a laboratory experiment was designed to evaluate the degradation of corrosion inhibitor by employing dominating individual species (*Serratia marcescens* ACE2, *Bacillus cereus* ACE4) and their role on corrosion process in petroleum products.

2. Materials and methods

2.1. Background information of the study

A cross-country pipeline in India, transports petroleum products such as kerosene, petrol and diesel. This pipeline has intermittent petroleum product delivery cum pressure booting stations at different locations. Severe corrosion and microfouling problems have been faced in the pipeline even though corrosion inhibitor was added. About 200–400 kg of muck (corrosion product) was received from a 200 km stretch of the pipeline within 30 days [15]. The corrosion product was pushed out of the pipeline by pigs (cylindrical device that moves with the flow of oil and cleans the pipeline interior) while cleaning the pipeline. The corrosion product samples were collected in sterile containers for microbial enumeration and identification. In the present study, commercially available water-soluble corrosion inhibitor used in petroleum transporting pipeline was evaluated to find out the nature of degradation, which was used in petroleum pipeline. The water-soluble corrosion inhibitor contains carboxylic acid and ester based compounds.

2.2. Microorganism

The strains *S. marcescens* ACE2 and *B. cereus* ACE4 [4] were used in this study were isolated from oil transporting pipeline of oil refineries in northwest India (the nucleotide sequences data has been deposited in GenBank under the sequence numbers DQ092416 and AY912105).

2.3. Composition of growth medium

The medium used for detecting the corrosion inhibitor degrading process by ACE4 was Bushnell–Hass broth (magnesium sulphate, 0.20 gm/l; calcium chloride, 0.02 gm/l; monopotassium phosphate, 1 gm/l; di-potassium phosphate, 1 gm/l; ammonium nitrate, 1 gm/l; ferric chloride, 0.05 gm/l, Hi-Media, Mumbai) and Bushnell–Hass agar. Three sets of erlenmeyer flasks were used for the inhibitor degradation studies using the selected bacterial strains.

2.4. Biodegradation of corrosion inhibitor and their characterization

Two sets of Erlenmeyer flasks containing 100 ml of the BH broth, 400 ppm of water-soluble corrosion inhibitor with ACE2 and ACE4 were inoculated. An uninoculated control flask was incubated parallelly to monitor abiotic losses of the corrosion inhibitors substrate. The flasks were incubated at 30 °C for 30 days in an orbital shaker (150 rpm). At the end of the 30 days of incubation period, the residual corrosion inhibitor for each

system of the entire flask was extracted with an equal volume of dichloromethane. Evaporation of solvent was carried out in a hot water bath at 40 °C. About 1 µl of the resultant solution was analyzed by Fourier transform infrared spectroscopy (FT-IR) and H^1 nuclear magnetic resonance spectroscopy (NMR). FT-IR spectrum (Nicolet Nexus 470) which was taken in the mid IR region of 400–4000 cm^{-1} with 16-scan speed. The samples were mixed with spectroscopically pure KBr in the ratio of 1:100 and the pellets were fixed in the sample holder, and the analysis was carried out. Infrared peaks localized at 2960 and 2925 cm^{-1} were used to calculate the CH_2/CH_3 ratio (absorbance) and functional group of both aliphatic and aromatic components present in water-soluble corrosion inhibitor. H^1 NMR (Bruker, 300 MHz) analysis was used to detect the protons of the nuclei in the diesel compound. The sample of diesel was dissolved using deuterated chloroform solvent. Tetramethyl silane (TMS) was used as a reference standard. The 1 µl of the resultant corrosion inhibitor solution was analyzed by Thermo Finnigan gas chromatography/mass spectrometry (trace MS equipped with a RTX-5 capillary column (30 m long \times 0.25 mm internal diameter) and high purity nitrogen as carrier gas. The oven was programmed between 80 and 250 °C at a heating temperature of 10 °C/min. The GC retention data of the inhibitor correspond to structural assignments done after NIST library search with a database and by mass spectra interpretation.

2.5. Inhibitor efficiency test

2.5.1. Rotating cage test

Corrosion inhibition efficiency was studied by rotating cage test [16, ASTM G170]. API 5LX grade steel (C, 0.29 max; S, 0.05 max; P, 0.04 max; Mn, 1.25 max) coupons of size 2.5 cm \times 2.5 cm were mechanically polished to mirror finish and then degreased using trichloro ethylene. Four coupons supported by polytetra fluoro ethylene (PTFE) disks were mounted at 55 mm apart on the rotatory rod. Holes were drilled in the top and bottom PTFE plates of the cage in order to increase the turbulence on the inside surface of the coupon. The rotatory rod runs at 200 rpm, which corresponds to a linear velocity of 0.53 m/s. In the present study, 500 ml of diesel with 2% water containing 120 ppm chloride as system I (control); 500 ml of diesel with 2% water containing 120 ppm chloride and 2 ml of mixed cultures of ACE2 and ACE4 as control system II; 500 ml of diesel with 2% water containing 120 ppm chloride and 100 ppm of corrosion inhibitor as system III; while 500 ml diesel with 2% of water containing 120 ppm chloride, 100 ppm of corrosion inhibitor inoculated with 2 ml of mixed cultures of ACE2 and ACE4 were used as the experimental system IV.

2.5.2. Flow loop test—for simulating the stratification of water in pipe flow

In order to simulate this sort up condition, a flow loop set-up was fabricated [16]. The flow loop system consists of a reservoir that maintains the solution under test, a pump with piping and bypass valve that controls the solution flow. Flow loop model has been made in the laboratory for creating stagnant water in the pipeline for simulating the field conditions.

The low velocity region is maintained in the cylindrical PVC pipe having a length of 20 cm and diameter of 12 cm. The suction line precedes the cylindrical device and the out let from the device is connected to the reservoir. The experimental set-up was washed by water thoroughly and dried well. The polished metal coupons were suspended in the set-up in the hook provided. In the present study, the following systems were made. The 8000 ml diesel + 2% water (120 ppm chloride) as system V (control); 8000 ml of diesel with 2% water containing 120 ppm chloride and 2 ml of mixed cultures of ACE2 and ACE4 system VI; 8000 ml of diesel with 2% water containing 120 ppm chloride and 100 ppm of water-soluble corrosion inhibitor as experimental system VII; 8000 ml diesel with 2% of water containing 120 ppm chloride, 100 ppm of water-soluble corrosion inhibitor inoculated with 2 ml of mixed cultures of ACE2 and ACE4 as system VIII.

After 7 days, the coupons were removed and washed in Clark's solution [17] for 1 min to remove the corrosion products and rinsed with sterile distilled water, dried. Final weights of the six coupons in each system were taken and the average corrosion rates were also calculated. The inhibition efficiency (IE) was calculated as follows:

$$\text{Inhibition efficiency (IE\%)} = \frac{W - W_{\text{inh}}}{W} \times 100$$

where W_{inh} and W are the values of the weight-loss of steel after immersion in solutions in the presence and in the absence of inhibitor, respectively.

2.6. Electrochemical methods for the evaluation of inhibitor

After the weight loss experiments (rotating test), electrochemical tests were carried out in a special cell containing aqueous medium collected from the rotating cage [18,4]. API 5LX steel coupon of size 1 cm² as working electrode, a standard calomel electrode (SCE) and platinum wire as counter electrode were employed for impedance and polarization studies. The Tafel polarization curves were obtained by scanning the potential from the open circuit potential towards 200 mV anodically and cathodically. The scan rate was 120 mV/min. Polarization measurements were carried out potentiodynamically using model PGP201, employing potentiostat with volta master-1-software.

2.7. Surface analysis study

To verify the adsorption of inhibitor on the metal surface in rotating cage test after 10 days, the film formed on the metal surface was carefully removed and dried, mixed thoroughly with potassium bromide (KBr) and made as pellets. These pellets are subjected to FT-IR spectra (Perkin-Elmer, Nicolet Nexus-470) to find out the protective film formed on the surface of the metal coupons. The surface morphological characteristics of the control and experimental carbon steel were observed under scanning electron microscope (SEM) Hitachi model S-3000H at magnification ranging from 50× to 200× operated at accelerating voltage of 25 kV.

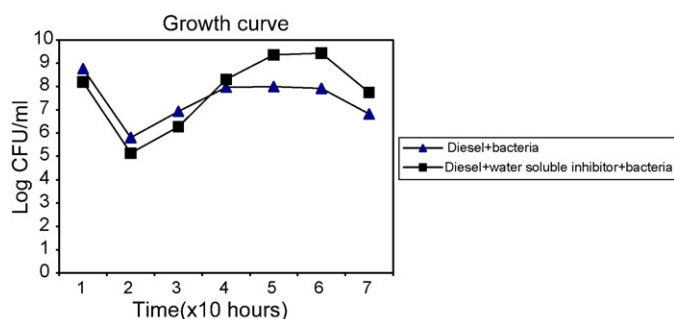


Fig. 1. Growth of mixed cultures (ACE2 and ACE4) in BH liquid medium in presence and absence of water-soluble corrosion inhibitor.

3. Results and discussions

In oil pipelines, water can also stratify at the bottom of line if the velocity is less than that required to entrain water and sweep it through the pipeline system. Liquids (hydrocarbon) stratify along the bottom of the pipe, with water forming a separate layer beneath the liquids where hydrocarbon degradation occurs at the interface easily by microbes. Hence, the role of bacteria on degradation and corrosion is an important area in petroleum product pipelines. The involvements of bacterial species on water-soluble corrosion inhibitor degradation and corrosion have been studied by various investigators [19,20,10,15,4]. It enlightens the role of bacterial species of *S. marcescens* ACE2 and *B. cereus* ACE4 on biodegradation of corrosion inhibitor in petroleum products and its influence on corrosion process in tropical countries.

3.1. Biodegradation analysis

3.1.1. Growth of bacteria

The total viable count of bacteria in the presence and in the absence of water-soluble corrosion inhibitor during degradation is presented in Fig. 1. The count is ranging between 10^6 and 10^8 in the presence of water-soluble inhibitor. In the absence of water-soluble corrosion inhibitor, the bacterial species ACE2 and ACE4 count decreased and found to be ranging between 2.13×10^6 and 2.38×10^8 CFU/ml, although initial load (2.14×10^8 CFU/ml) was same in all the systems. The proliferation of bacteria is higher in the presence of water-soluble inhibitor compared to absence of inhibitor. It could be explained that ACE2 and ACE4 utilizes the inhibitor as organic source with inorganic nutrients from the BH media for their proliferation. It indicates that water-soluble corrosion inhibitor enhanced the proliferation of bacteria (ACE2 and ACE4).

3.1.2. Degradation of water-soluble corrosion inhibitor

FT-IR spectrum of water-soluble corrosion inhibitor (Fig. 2(a)) shows OH stretching bands in the range of 3429 cm^{-1} . It is due to the hydroxyl group present in the inhibitor. The methyl (CH_3) and methylene (CH_2) protons are observed in the range of 2959 and 2873 cm^{-1} . The strong band at 1709 cm^{-1} is due to C=O (carbonyl group) stretching band, it indicates the presence of carboxylic acid group in inhibitor. The peaks at 1459 cm^{-1} and

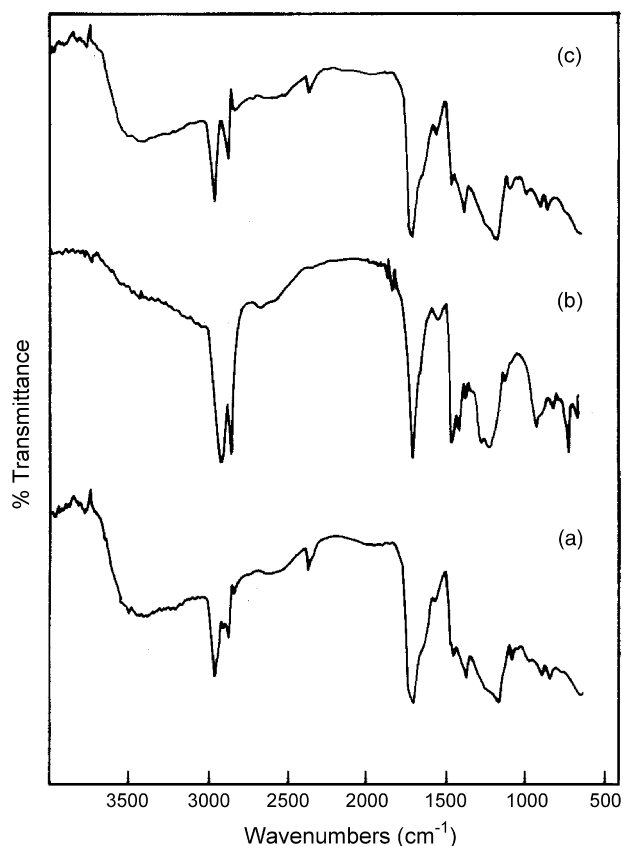


Fig. 2. Fourier transform infrared spectrum: (a) water-soluble corrosion inhibitor (uninoculated system – control), (b) inoculated with *Serratia marcescens* ACE2, and (c) inoculated with *Bacillus cereus* ACE4.

1378 cm^{-1} are due to C–H def for methyl group. The peaks at 1173 and 1078 cm^{-1} indicate the presence of C=O stretching for ester (C–O–C) group. The peaks at 897 and 839 cm^{-1} indicate the sub substituted benzene ring.

In presence of *S. marcescens* ACE2 with water-soluble corrosion inhibitor (Fig. 2(b)), the methyl (CH_3) and methylene (CH_2) protons are observed in the range of 2916 and 2852 cm^{-1} , respectively. The olefinic (=C–H) overtones band is observed in the range of 1917 cm^{-1} . The strong band at 1706 cm^{-1} is due to C=O stretching band for acid group. The peaks at 1546, 1458 and 1412 cm^{-1} are due to carboxylate anion (COO^-) bands. A peak at 1372 cm^{-1} indicates the presence of C–H def for methyl group. The peaks at 1237 and 1113 cm^{-1} are C=O stretching for ester group. A peak at 933 cm^{-1} indicates the presence of substituted benzene ring due to the substitution reaction induced by bacteria and a peak at 723 cm^{-1} is due to olefinic or aromatic C–H out of plane bending band. FT-IR spectrum reveals that the oxygen substitution reaction is taking place during degradation, due to the bacterial activity (oxygenase enzyme). The hydroxyl peak at 3429 cm^{-1} could not be observed in presence of ACE2 when compared to control (without bacteria). It reveals that the inhibitor contains carboxylic acid group and this acid group is cleaved to carboxylate anion (COO^-). In presence of *B. cereus* ACE4 with water-soluble corrosion inhibitor (Fig. 2(c)), OH stretching band is observed in the range of 3430 cm^{-1} . The methyl (CH_3) and methylene (CH_2) protons can be noticed at

the peaks of 2959, 2873 and 2832 cm^{-1} , respectively. The strong band at 1706 cm^{-1} is due to C=O stretching band for acid group. The peaks at 1554 and 1458 cm^{-1} are due to COO^- (carboxylate anion) bands. Another peak at 1378 cm^{-1} indicating the presence of C–H def for methyl group. The peaks at 1171 and 1077 cm^{-1} indicate the presence of C=O stretching for ester group. The peak at 897 and 839 cm^{-1} indicates the presence of substituted benzene ring. In presence of bacterial species ACE2 and ACE4, a new peak can be noticed at 1554 cm^{-1} , 1458 cm^{-1} and 1378 cm^{-1} , indicates the carboxylate anion (COO^-). It reveals that due to bacterial activity, the acid group is cleaved and produced as the carboxylate anions. The absence of hydroxyl peak (OH) in the inhibitor during degradation, which indicates that the ACE2 is a more degrader than ACE4.

NMR spectrum of water-soluble corrosion inhibitor shows the characteristic band in Fig. 3(a). The peak at 7.05 ppm is due to aromatic C–H protons. The multiplet peaks at 4.89–5.29 ppm is due to oxygen-included protons. The CH_2 aliphatic protons can be observed between 2.57 and 2.59 ppm. Another acetylenic proton peak is observed between 2.19 and 2.29 ppm. The aliphatic methylene (CH_2) peaks are noticed at 1.1 and 1.6 ppm and the methyl proton peaks are observed at 0.86 ppm. It reveals the presence of aliphatic and aromatic protons based compounds in water-soluble corrosion inhibitor. In presence of bacteria ACE2 (Fig. 3(b)), the two types of olefinic protons can be observed at 5.35, 5.33 and 5.28 ppm. The disappearance of aromatic protons at 7 ppm reveals that bacteria consumed the aromatic compound. The CH_2 proton peak is observed in the range of 1.85 to 2.51 ppm as a multiplet peak. An aliphatic peak at 1.58 and methyl protons at 0.28 and 0.97 can be noticed. In presence of bacteria ACE4 (Fig. 3(c)), the two types of acidic protons can be observed at 5.35, 5.33 and 5.28 ppm. The peak at 7 ppm indicates the presence aromatic protons. The acetylene proton peak is observed in the range of 1.98–2.89 ppm as a multiplet peak and aliphatic peak at 1.58 and methyl protons can be noticed at 0.86 and 1.19. The intensity of aliphatic proton peaks at (1.58, 0.97 and 0.28) is lesser in ACE2 when compared to ACE4. It reveals that ACE2 consumes high quantity of hydrogen in the 30 days period of degradation. ACE2 consumes both aliphatic and aromatic hydrocarbons present in the inhibitor but ACE4 consumes only aliphatic protons as a food source which supports the FT-IR spectrum.

The GC retention data of the water-soluble inhibitor correspond to structural assignments done after NIST library search with a database and the mass spectra interpretations are presented in Table 1. From the GC–MS analysis (Fig. 4), it can be observed that the water-soluble corrosion inhibitor (uninoculated system) consists two major components which are (1) 2-docene-1-yl(–) succinic anhydride and (2) bis(2-ethylhexyl) phthalate [1,2-benzene dicarboxylic acid bis(2-ethylhexyl) ester] and the molecular weight is about 266 and 390, respectively.

In presence of ACE2 (Fig. 5), the new compounds can be observed at 1.69, 3.78, 5.40, 6.54, 7.43, 7.59, 8.38, 9.19, 9.77, 9.94, 16.18 min retention time which indicate the presence of benzene,1,2,3,5-tetramethyl, naphthalene,2-methyl, 1,1'-biphenyl,2-methyl, benzene,1-methyl-2-(phenylmethyl), benzene,

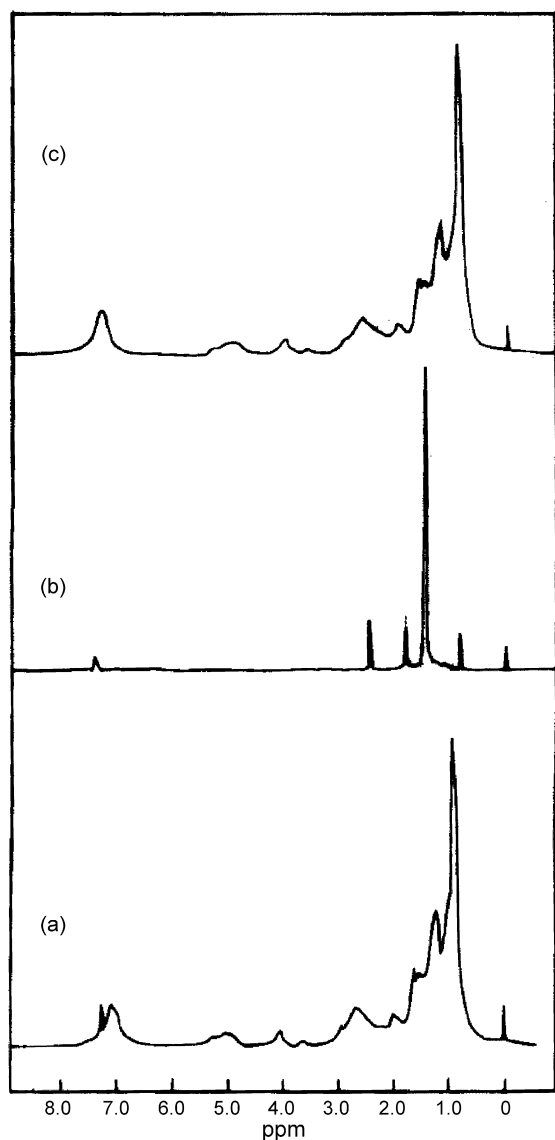


Fig. 3. H^1 NMR spectrum: (a) water-soluble corrosion inhibitor (uninoculated system – control), (b) inoculated with *S. marcescens* ACE2, and (c) inoculated with *B. cereus* ACE4.

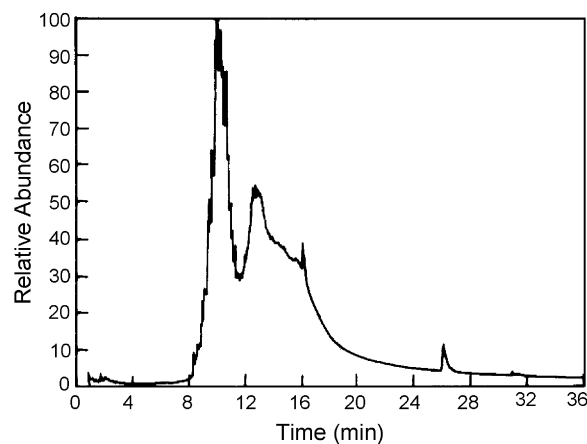


Fig. 4. GC–MS spectrum of pure water-soluble corrosion inhibitor.

1,1'-methylenebis[4-methyl]benzene, 1,1'-methylenebis[4-methyl], 3,5,3',5'-tetramethylbiphenyl, 1,5,6,7-tetramethyl-3-phenylbicyclo[3,2,0]hepta-2,6-diene, 1,5,6,7-tetramethyl-3-phenylbicyclo[3,2,0]hepta-2,6-diene, 1,5,6,7-tetramethyl-3 phenyl bicyclo[3,2,0]hepta-2,6-diene, bis(2-ethylhexyl) phthalate, respectively. It can be explained that it is due to the decomposition or degradation of aliphatic and aromatic compounds present in the inhibitor (Table 2). The high concentration (relative abundance—100%) of benzene,1,2,3,5-tetramethyl in presence of ACE2 indicates utility of the high molecular weight of aliphatic and aromatic components present in the water-soluble corrosion inhibitor. The molecular weight of the water-soluble corrosion inhibitor highly reduced by ACE2 from 392 to 142.

In presence of ACE4 (Fig. 6) the presence of 2-docene-1-yl(–) succinic anhydride but the intensity of the peak is remarkably reduced when compared to control (Table 3). The new compound [3',8,8'-trimethoxy-3-piperidyl-2,2'-binaphthalene-1,1',4,4'-tetrone] was observed at 16.20 min retention time. It indicates that bis(2-ethylhexyl) phthalate [1,2-benzene dicarboxylic acid bis(2-ethylhexyl) ester] is the major component present in water-soluble corrosion inhibitor and is completely consumed by ACE4. Another significant observation is the for-

Table 1
GC–MS data of pure water-soluble corrosion inhibitor

Retention time (min)	Compound	Molecular formula	Molecular weight
9.03	2-Docene-1-yl(–) succinic anhydride	$C_{16}H_{26}O_3$	266
9.30	2-Docene-1-yl(–) succinic anhydride	$C_{16}H_{26}O_3$	266
9.52	2-Docene-1-yl(–) succinic anhydride	$C_{16}H_{26}O_3$	266
9.69	2-Docene-1-yl(–) succinic anhydride	$C_{16}H_{26}O_3$	266
10.01	2-Docene-1-yl(–) succinic anhydride	$C_{16}H_{26}O_3$	266
10.07	2-Docene-1-yl(–) succinic anhydride	$C_{16}H_{26}O_3$	266
10.24	2-Docene-1-yl(–) succinic anhydride	$C_{16}H_{26}O_3$	266
10.12	2-Docene-1-yl(–) succinic anhydride	$C_{16}H_{26}O_3$	266
10.43	2-Docene-1-yl(–) succinic anhydride	$C_{16}H_{26}O_3$	266
11.10	2-Docene-1-yl(–) succinic anhydride	$C_{16}H_{26}O_3$	266
11.28	2-Docene-1-yl(–) succinic anhydride	$C_{16}H_{26}O_3$	266
12.89	2-Docene-1-yl(–) succinic anhydride	$C_{16}H_{26}O_3$	266
13.66	2-Docene-1-yl(–) succinic anhydride	$C_{16}H_{26}O_3$	266
16.18	Bis(2-ethylhexyl) phthalate [1,2-benzene dicarboxylic acid bis(2-ethylhexyl) ester]	$C_{24}H_{38}O_4$	390

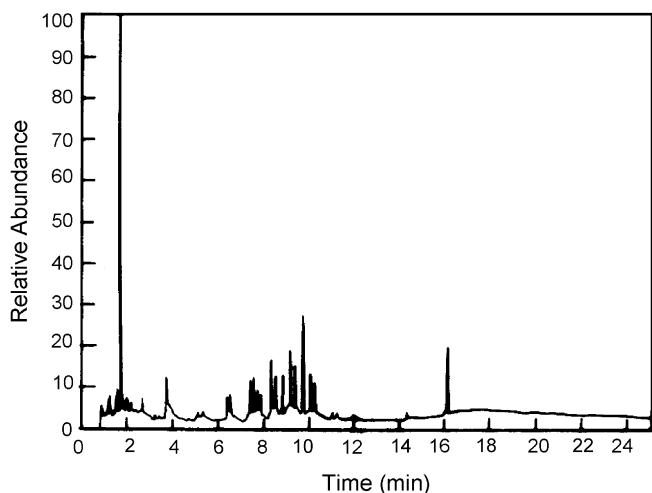


Fig. 5. GC–MS spectrum of pure water-soluble corrosion inhibitor inoculated with ACE2.

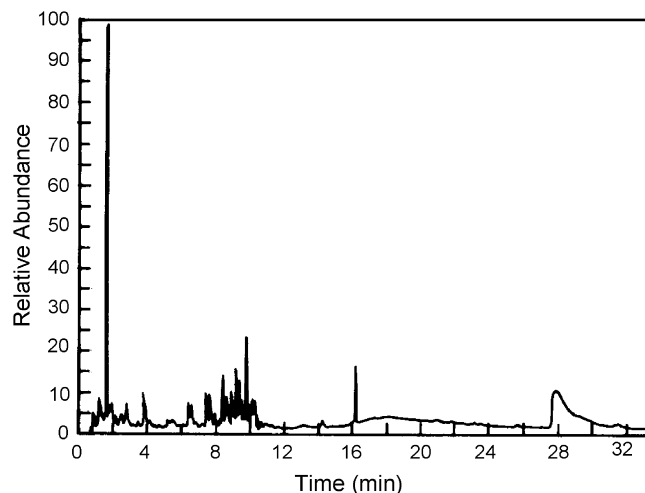


Fig. 6. GC–MS spectrum of pure water-soluble corrosion inhibitor inoculated with ACE4.

mation of new compound benzene,1,2,3,5,tetramethyl at 1.69 retention time in presence of both bacterial species (ACE2 and ACE4). In presence of ACE4 there is no change in the compound 2-docene-1-yl(–) succinic anhydride present as inhibitor.

The present study reveals that, the isolates have the capacity to degrade both the aromatic and aliphatic hydrocarbon present in the water-soluble corrosion inhibitor in petroleum product pipeline. Videla et al. [10] also noticed microbial degradation of film forming inhibitor and observed that *Pseudomonas* sp. isolated from injection water degraded several aromatic compounds and generated energy for its metabolic activity. They also suggested that dimethylamine, imidazoline, morpholine, cyclo hexylamine and quaternary ammonium compounds are biodegradable. The present study also supports the observation made by Rajasekar et al. [4] that the strain ACE4 has the high preference to degrade both aliphatic and aromatic components in a inhibitor.

FT-IR spectrum reveals that the oxygen substitution reaction has taken place during degradation, which is due to the bacterial activity (oxygenase enzyme). The hydroxyl peak at 3429 cm^{-1} could not be observed in presence of ACE2 when compared to control (without bacteria). It reveals that the inhibitor contains

carboxylic acid group, this acid group is cleaved into carboxylate anion (COO^-) and hydrogen was consumed by bacteria (ACE2). The absence of hydroxyl peak (OH) in the inhibitor during degradation indicates that the ACE2 is more degrader than ACE4. The NMR results reveal that the intensity of aliphatic proton peaks at (1.58, 0.97 and 0.28) is lesser in ACE2 when compared to ACE4. It reveals that ACE2 consumes high quantity of hydrogen in the 30 days period of degradation. ACE2 consumes both aliphatic and aromatic hydrocarbons present in the inhibitor but ACE4 consumes only aliphatic protons as a food source, which supports the FT-IR spectrum. GC–MS results conclude that the molecular weight of the water-soluble corrosion inhibitor is highly reduced by ACE2 from 392 to 142. ACE4 shows the presence of 2-docene-1-yl(–) succinic anhydride but the intensity of the peak is remarkably reduced when compared to control. The degraded products viz., 3',8,8'-trimethoxy-3-piperidyl-2,2'-binaphthalene-1,1',4,4'-tetrone was observed at 16.20 min retention time. Another significant observation is the formation of new compound benzene,1,2,3,5,tetramethyl at 1.69 min retention time in presence of both the bacterial species (ACE2 and ACE4). In presence of ACE4 there is no change in the compound 2-docene-1-yl(–) succinic anhydride present in the inhibitor.

Table 2

GC–MS data of water-soluble corrosion inhibitor after 30 days of inoculation with strain *Serratia marcescens* ACE2

Retention time (min)	Compound	Molecular formula	Molecular weight
1.69	Benzene,1,2,3,5-tetramethyl	$\text{C}_{10}\text{H}_{14}$	134
3.78	Naphthalene,2-methyl	$\text{C}_{11}\text{H}_{10}$	142
5.40	1,1'-Biphenyl,2-methyl	$\text{C}_{13}\text{H}_{12}$	168
6.54	Benzene,1-methyl-2-(phenylmethyl)	$\text{C}_{14}\text{H}_{14}$	182
7.43	Benzene,1,1'-methylenebis[4-methyl]	$\text{C}_{15}\text{H}_{16}$	196
7.59	Benzene,1,1'-methylenebis[4-methyl]	$\text{C}_{15}\text{H}_{16}$	196
8.38	3,5,3',5'-Tetramethylbiphenyl	$\text{C}_{16}\text{H}_{18}$	210
9.19	1,5,6,7-Tetramethyl-3-phenylbicyclo[3,2,0]hepta-2,6-diene	$\text{C}_{17}\text{H}_{20}$	224
9.77	1,5,6,7-Tetramethyl-3-phenylbicyclo[3,2,0]hepta-2,6-diene	$\text{C}_{17}\text{H}_{20}$	224
9.94	1,5,6,7-Tetramethyl-3-phenylbicyclo[3,2,0]hepta-2,6-diene	$\text{C}_{17}\text{H}_{20}$	224
16.18	Bis(2-ethylhexyl) phthalate	$\text{C}_{24}\text{H}_{38}\text{O}_4$	390

Table 3
GC–MS data of water-soluble corrosion inhibitor after 30 days of inoculation with strain *Bacillus cereus* ACE4

Retention time (min)	Compound	Molecular formula	Molecular weight
9.06	2-Docene-1-yl(–) succinic anhydride	C ₁₆ H ₂₆ O ₃	266
9.34	2-Docene-1-yl(–) succinic anhydride	C ₁₆ H ₂₆ O ₃	266
9.54	2-Docene-1-yl(–) succinic anhydride	C ₁₆ H ₂₆ O ₃	266
9.83	2-Docene-1-yl(–) succinic anhydride	C ₁₆ H ₂₆ O ₃	266
10.03	2-Docene-1-yl(–) succinic anhydride	C ₁₆ H ₂₆ O ₃	266
10.26	2-Docene-1-yl(–) succinic anhydride	C ₁₆ H ₂₆ O ₃	266
10.41	2-Docene-1-yl(–) succinic anhydride	C ₁₆ H ₂₆ O ₃	266
11.14	2-Docene-1-yl(–) succinic anhydride	C ₁₆ H ₂₆ O ₃	266
11.30	2-Docene-1-yl(–) succinic anhydride	C ₁₆ H ₂₆ O ₃	266
10.85	2-Docene-1-yl(–) succinic anhydride	C ₁₆ H ₂₆ O ₃	266
16.20	3',8,8'-Trimethoxy-3-piperidyl-2,2'-binaphthalene-1,1',4,4'-tetrone	C ₂₈ H ₂₅ NO ₇	487

Table 4
Corrosion rates of API 5LX with water-soluble corrosion inhibitor in rotating cage method

S. no.	System	Weight loss (mg)	Corrosion rate (mm/year)	Inhibition efficiency (%)
1	System I (control): 500 ml of diesel + 2% water (120 ppm chloride)	26.5	0.3262	–
2	System II: 500 ml of diesel + 2% water (120 ppm chloride) + bacterial culture	41.7	0.5133	–
3	System III: 500 ml of diesel + 2% water (120 ppm chloride) + water-soluble inhibitor (100 ppm)	8.9	0.1095	66.43
4	System IV: 500 ml of diesel + 2% water (120 ppm chloride) + bacterial culture (ACE2 and ACE4) + water-soluble inhibitor (100 ppm)	12.6	0.1551	52.45

3.2. Weight loss studies

3.2.1. Inhibitor efficiency

3.2.1.1. *Rotating cage test.* The inhibition efficiency (IE) of water-soluble corrosion inhibitor is presented in Table 4. The corrosion rate of API 5 LX in control system (without inoculums) is 0.3262 mm/year in 168 h. In presence of microbes and absence of water-soluble corrosion inhibitor (system II), the corrosion rate is about 0.5133 mm/y when compared to the absence of microbes. The water-soluble corrosion inhibitor gives inhibition efficiency of about 66%. In presence of water-soluble corrosion inhibitor along with bacteria, the inhibition efficiency of about 52%. The present observation reveals that bacteria reduces the efficiency of water-soluble corrosion inhibitor about 12%.

3.2.1.2. *Flow loop test.* The inhibition efficiency (IE) of water-soluble corrosion inhibitor is presented in Table 5. The corrosion rate of API 5LX in control system (without inoculums) is 0.0923 mm/year in 168 h. In presence of microbes and absence

of water-soluble corrosion inhibitor (system II), the corrosion rate is higher in the range of 0.4874 mm/y when compared to the absence of microbes. The water-soluble corrosion inhibitor gives inhibition efficiency of about 36%. In presence of water-soluble corrosion inhibitor along with bacteria, the inhibition efficiency is about 15%. The present observation reveals that bacteria reduce the efficiency of water-soluble corrosion inhibitor to about 21%.

The weight loss data reveals that bacterial culture reduces the efficiency of inhibitor. It is due to the degradation of inhibitor in the system. The reduction in efficiency of inhibitor is higher in flow loop method when compared to rotating cage method. It indicates that the water stagnant point in the flow system may enhance the inhibitor degradation, and affect the inhibition efficiency.

3.2.2. Electrochemical studies

3.2.2.1. *Rotating cage method.* The polarization results for API 5LX in water collected from rotating cage are presented in

Table 5
Corrosion rates of API 5LX with water-soluble corrosion inhibitor in flow loop method

S. no.	System	Weight loss (mg)	Corrosion rate (mm/year)	Inhibition efficiency (%)
1	System V (control): 8000 ml of diesel + 2% water (120 ppm chloride)	7.56	0.0923	–
2	System VI: 8000 ml of diesel + 2% water (120 ppm chloride) + bacterial culture (ACE2 and ACE4)	39.6	0.4874	–
3	System VII: 8000 ml of diesel + 2% water (120 ppm chloride) + water-soluble inhibitor (100 ppm)	4.8	0.0590	36.40
4	System VIII: 8000 ml of diesel + 2% water (120 ppm chloride) + bacterial culture (ACE2 and ACE4) + water-soluble inhibitor (100 ppm)	6.43	0.0791	14.62

Table 6
Polarization data for API 5LX with water-soluble corrosion inhibitor in rotating cage method

S. no.	System	E_{corr} (mV)	B_a (mV/decade)	B_c (mV/decade)	I_{corr} (A/cm ²)
1	System I: 500 ml diesel + 2% water (120 ppm chloride)	−580	142	645	4.75×10^{-6}
2	System II: 500 ml diesel + 2% water (120 ppm chloride) + bacterial cultures (ACE2 and ACE4)	−240	192	190	1.80×10^{-9}
3	System III: 500 ml diesel + 2% water (120 ppm chloride) + water-soluble inhibitor 100 ppm	−488	65	169	1.13×10^{-8}
4	System VI: 500 ml diesel + 2% water (120 ppm chloride) + bacterial cultures (ACE2 and ACE4) + water-soluble inhibitor 100 ppm	−356	152	204	2.51×10^{-8}

Table 6 and Fig. 7. The corrosion potential (E_{corr}) for API 5LX steel in control system is −580 mV versus SCE (standard calomel electrode), while adding water-soluble corrosion inhibitor the corrosion potential shifted to −488 mV. Besides, the corrosion current in control system is 4.75×10^{-6} A/cm² while, adding water-soluble corrosion inhibitor the corrosion current is suppressed where the current is in the range of 1.13×10^{-8} A/cm². But in presence of bacterial system, the potential is about −240 mV and the corrosion current is reduced to 1.80×10^{-9} A/cm² and bacteria along with water-soluble corrosion inhibitor the corrosion current is 2.51×10^{-8} A/cm² and the potential is −356 mV versus SCE. The result indicates that the inhibitor reduces the current significantly without bacteria. Bacteria shift the potential to positive side, indicates that bacteria adsorbs on the metal surface and improves the passivity and suppresses the corrosion current.

But in presence of bacteria the inhibitor does not give significant reduction in corrosion current. It reveals that bacteria accelerate corrosion and it interferes the inhibitive action of inhibitor biodegradation. The corrosion potential (E_{corr}) indicates the shifts of open circuit potential (OCP) from −580 to −488 mV versus SCE in presence of inhibitor while in presence of bacteria the potential goes to negative side. It also reveals that the bacterial contamination interferes the inhibitive action. It can be explained that the biodegraded products dissolve in water and supply electron to metal surface, which accelerates

the cathodic process. In presence of water-soluble corrosion inhibitor, the dissolved amine proton in water may decrease the cathodic current where as the anodic current is increased by the metabolic products of the bacteria dissolved in the contaminated water.

3.2.2.2. *Flow loop method.* The polarization data for API 5LX steel for the control system and the inhibitor added system is presented in Fig. 8 and Table 7. In control system (system V), the corrosion potential (E_{corr}) is about −350 mV, while adding inhibitor, bacterial cultures and bacterial cultures with inhibitor the potential shifted to −307, −605 and −614 mV, respectively. The nature of curves indicate that the inhibitor suppresses both anodic and cathodic reaction and it can be claimed as mixed inhibitor. The corrosion current is about 1.57×10^{-7} A/cm² in control system whereas in the presence of inhibitor, bacteria and bacteria with inhibitor the corrosion current is 9.82×10^{-9} , 1.05×10^{-5} and 1.52×10^{-7} A/cm², respectively.

In presence bacteria, the corrosion current (I_{corr}) is increased when compared to control (system V), which contradicts with rotating cage method. It can be explained that the water contact in stagnant system on coupons may be the reason for the high corrosion rate and detailed study is needed for this stagnant model. In system VIII, the corrosion current I_{corr} is more or less same as control (system V), which also indicates the bacterial influence on inhibition activity.

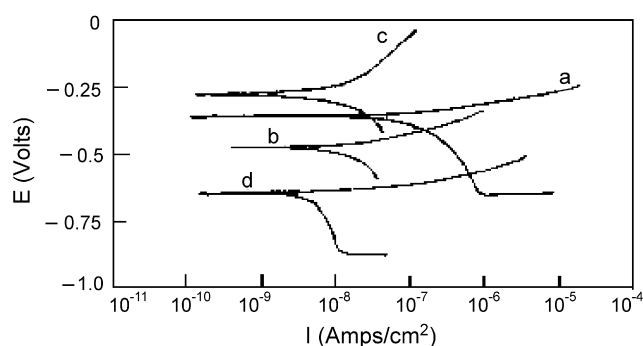


Fig. 7. Polarization curve for water-soluble corrosion inhibitor in rotating cage system: (a – system I): 500 ml diesel + 2% water containing 120 ppm chloride (control); (b – system II): 500 ml diesel + 2% water containing 120 ppm chloride + 2 ml bacterial culture (ACE2 and ACE4); (c – system III): 500 ml diesel + 2% water containing 120 ppm chloride + 100 ppm water-soluble inhibitor; (d – system IV): 500 ml diesel + 2% water containing 120 ppm chloride + 100 ppm of water-soluble inhibitor + 2 ml bacterial culture (ACE2 and ACE4).

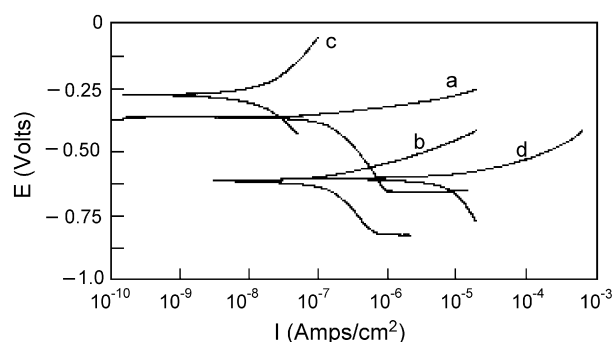


Fig. 8. Polarization curve for API 5LX in diesel water system, in presence and absence of water-soluble corrosion inhibitor in flow loop method: (a) system V: 8000 ml diesel + 2% water (120 ppm chloride); (b) system VI: 8000 ml diesel + 2% water + 5 ml mixed cultures (ACE2 and ACE4); (c) system VII: 8000 ml diesel + 2% water (120 ppm chloride) + water-soluble corrosion inhibitor 100 ppm; (d) system VIII: 8000 ml diesel + 2% water + water-soluble corrosion inhibitor 100 ppm + 5 ml mixed cultures (ACE2 And ACE4).

Table 7
Polarization data for API 5LX with water-soluble corrosion inhibitor in flow loop method

S. no.	System	E_{corr} (mV)	B_a (mV/decade)	B_c (mV/decade)	I_{corr} (A/cm ²)
1	System V: 8000 ml diesel + 2% water (120 ppm chloride)	-350	36	376	1.58×10^{-7}
2	System VI: 8000 ml diesel + 2% water (120 ppm chloride) + bacterial culture (ACE2 and ACE4)	-605	102	350	1.05×10^{-5}
3	System VII: 8000 ml diesel + 2% water (120 ppm chloride) + water-soluble inhibitor 100 ppm	-307	213	163	9.82×10^{-9}
4	System VIII: 8000 ml diesel + 2% water (120 ppm chloride) + bacterial culture (ACE2 and ACE4) + water-soluble inhibitor 100 ppm	-614	87	292	1.52×10^{-7}

3.3. Surface analysis

3.3.1. FT-IR studies

Fig. 9(a) shows the FT-IR spectrum of corrosion product sample collected from rotating cage system without inhibitor (system I). The peak at 3133 cm^{-1} indicates the presence of OH stretch. The peaks at 2922 and 2852 cm^{-1} indicate the presence of CH aliphatic stretch. The peaks at 1576 and 1457 cm^{-1} indicate the C=C aromatic nuclei. The peak at 1378 cm^{-1} indicates the presence of CH def for methyl group. The peaks at 1124 and 1019 cm^{-1} indicate the C=O (carbonyl group) stretch for C–O–C group. It may be ester peak. The peaks at 880 and 745 cm^{-1} indicate the presence of substituted benzene peak.

Fig. 9(b) shows the FT-IR spectrum of muck sample collected from the rotating cage system with inhibitor (system III). The peaks at 2925 and 2855 cm^{-1} indicate the presence of CH aliphatic group. The peak at 1633 cm^{-1} indicates C=C

conjugated diene. A peak at 1443 cm^{-1} indicates the CH def for methyl group. Another peak at 1020 cm^{-1} indicates the CO stretch for C–O–C group.

Fig. 9(c) shows the FT-IR spectrum of muck sample collected from the rotating cage system with bacterial culture (system II). A peak at 3342 cm^{-1} indicates the presence of OH stretch. The peaks at 2925 and 2859 cm^{-1} indicate the presence of CH aliphatic stretch. A peak at 1725 cm^{-1} indicates the presence of C=O (Carbonyl group). The peak at 1631 cm^{-1} indicates the presence of C=C conjugated diene. The peaks at 1461 cm^{-1} and 1376 cm^{-1} indicate the CH def for methyl group. The peaks at 1168 and 1034 cm^{-1} indicate the presence of C=O (carbonyl group) stretch for C–O–C group. The peaks at 809 and 742 cm^{-1} indicate the presence of substituted benzene compounds.

Fig. 9(d) shows the FT-IR spectrum of muck sample collected from the rotating cage system inhibitor with bacterial culture system (system IV). A peak at 3133 cm^{-1} indicates the presence of OH stretch. The peaks at 2925 and 2889 cm^{-1} indicate the presence of CH aliphatic stretch. The peaks at 1805 , 1776

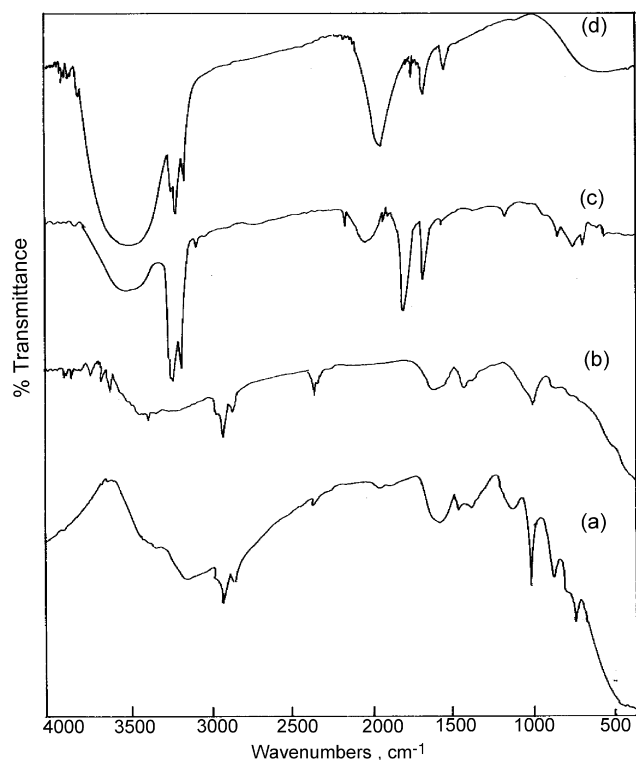


Fig. 9. FT-IR spectrum for surface film collected in rotating cage method: (a) system I; (b) system III; (c) system I; (d) system IV.

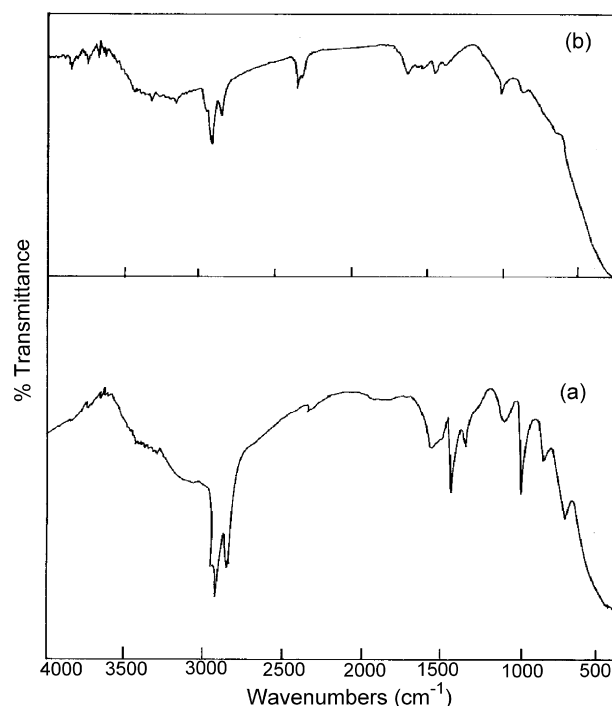


Fig. 10. FT-IR spectra for surface film collected in flow loop method: (a) system V; (b) system VII.

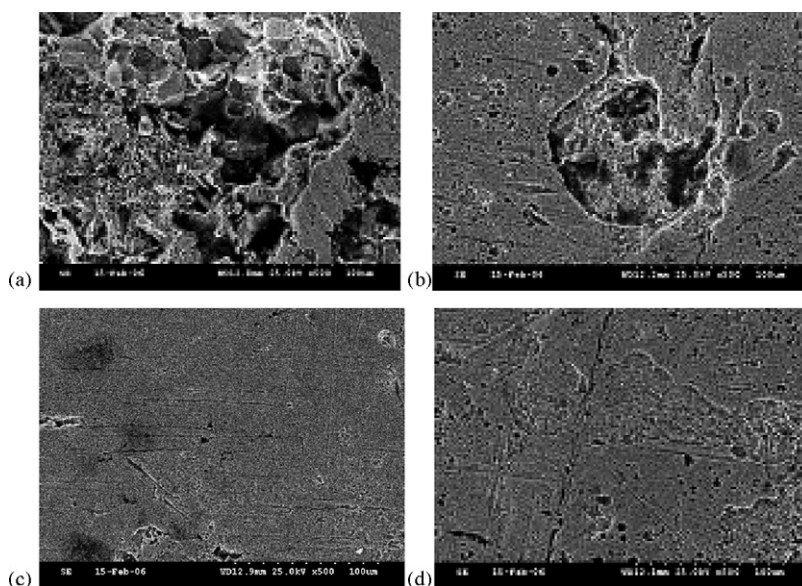


Fig. 11. Scanning electron micrograph of API 5LX in: (a) system I; (b) system II; (c) system III; (d) system VI.

and 1754 cm^{-1} indicate the presence of C=O group. A peak at 1632 cm^{-1} indicates the presence of conjugated diene. A peak at 1538 cm^{-1} indicates the presence of C=C aromatic nuclei. The peaks at 744 and 629 cm^{-1} indicate the presence of C–Cl peak.

Fig. 10(a) shows the FT-IR spectrum of corrosion product collected from flow loop system without inhibitor (system V). The peak at 3331 cm^{-1} indicates the presence of OH stretch. The peaks at 2924 and 2853 cm^{-1} indicate the presence of CH aliphatic stretch. The peak at 1641 cm^{-1} indicates the presence of C=C conjugated diene. The peaks at 1019 cm^{-1} indicates the presence of C=O (carbonyl group) stretch for C–O–C group. FT-IR spectrum of inhibitor added system (system VII) (Fig. 10(b)) reveals that the adsorption of inhibitor on the metal surface could not be noticed at 1557 , 1550 and 1470 cm^{-1} . It may be due to the activity of bacteria in flow system.

The commercially available inhibitor consists of carboxylic acid and ester based compounds. While adding inhibitor in the flow loop method (Fig. 10(a) and (b)), both the components adsorb on the metal surface and inhibit the corrosion. Besides, it is well known that ester is a preservative for diesel, which also adsorb on the metal surface in the lab conditions. But in the presence of inhibitor with bacterial culture inoculated system, the carboxylic anion [COO^- , 1567 , 1550 , 1470 cm^{-1}] could not be adsorbed on the metal surface. Besides, due to the bacterial adhesion on the metal surface, C=O stretch amide group can be noticed at 1805 and 1776 cm^{-1} on the metal surface. It reveals that the bacteria form as biofilm with amide group (–CONH–). It is also possible that the biofilm degrade the acid group (COO^-) to amide group (–CONH–). The amide formation may be due to the organic complex between biofilm (Amino acids) and corrosion inhibitor. Hence, the efficiency of inhibitor is reduced about 21% in rotating cage method and 60% in flow loop method. The present observation supports the observation made by Rajasekar et al. [4].

3.3.2. SEM analysis

SEM picture of the metal surface was recorded before and after treatment with inhibitor (Fig. 11a–d). As seen from the picture in absence of inhibitor (Fig. 11a) pitting type of corrosion was observed whereas in presence of inhibitor there was only very mild and uniform corrosion (Fig. 11c). The pitting type corrosion has taken place in presence of bacterial culture alone and along with inhibitor system (Fig. 11b–d).

4. Conclusions

1. The selection of inhibitor in petroleum product pipeline is an important factor that the inhibitor should not be soluble in water.
2. Microbial activity can result in inhibitor degradation, which would lead to unacceptable level of turbidity, corrosion of pipeline and souring of stored products. Hence, the quality of degradation characteristics should be checked by microbes collected at pipeline.
3. The FT-IR, NMR and GC–MS results reveal that *S. marcescens* ACE2 is major aliphatic and aromatic hydrocarbon degrader when compared to *B. cereus* ACE4.
4. The weight loss data and electrochemical studies reveal that bacterial culture reduces the efficiency of inhibitor. It is due to the degradation of inhibitor in the system. The reduction in efficiency of inhibitor is higher in flow loop method when compared to rotating cage method. It indicates that the water stagnant point in the flow system may enhance the inhibitor degradation, which may affect the inhibition efficiency.
5. While administering the inhibitors, the pipeline should be pigged. Immediately after pigging the line, a higher concentration of the micro biocide can be added followed by periodical additions at lower concentrations (shock treatment). Besides, the persistency and the level of inhibitor should be checked by collection of samples periodically at

various pumping stations. The carboxylate anion adsorption level is the major factor in internal pipeline corrosion.

Acknowledgements

The authors wish to express their thanks to The Director, CECRI, Karaikudi-6 for his kind permission. One of the authors N. Muthukumar thanks CSIR for the award of Senior Research Fellowship. The authors thank to Mr. A. Rajasekar, SRF for providing the identified bacterial species collected from a petroleum product pipeline and grateful to Dr. S. Sathiyarayanan for his kind help in electrochemical techniques.

References

- [1] D.H. Pope et al., Mitigation Strategies for Microbiologically Influenced Corrosion in Gas Industry Facilities, CORROSION/89, Paper No. 192, NACE, Houston, TX, 1989.
- [2] L.H. Lin, et al., Org. Geochem. 4 (5) (1989) 511–523.
- [3] H. Kobayashi, B.E. Rittman, Environ. Sci. Technol. 16 (3) (1982) 170–183.
- [4] A. Rajasekar, S. Maruthamuthu, N. Palaniswamy, A. Rajendran, Biodegradation of corrosion inhibitors and their influence on petroleum product pipeline, Microbiol. Res., in press.
- [5] F.M. Bento, C.C. Gaylarde, Biodeterioration of stored diesel oil: studies in Brazil, Int. Biodeter. Biodegr. 47 (2001) 107–112.
- [6] J.L. Shennan, Control of microbial contamination of fuels in storage, in: D.R. Houghton, R.N. Smith, H.O.W. Egging (Eds.), Biodeterioration, Elsevier, Barking, 1988, pp. 248–254.
- [7] H.A. Videla, W.G. Characklis, Biofouling and microbially influenced corrosion, Int. Biodeter. Biodegr. 29 (1992) 195–212.
- [8] D.A. Jones, P.S. Amy, A thermodynamic interpretation of microbially influenced corrosion, Corrosion 58 (2002) 638–645.
- [9] B. Little, R. Ray, A perspective on corrosion inhibition by biofilms, Corrosion 58 (2002) 424–428.
- [10] H.A. Videla, S.G. G. De Saravia, P.S. Guimet, P. Allegreti, J. Furlong, Microbial degradation of film-forming inhibitors and its possible effects on corrosion inhibition performance corrosion/2000, paper no.00386 (Houston, TX, NACE International, 2000).
- [11] P. Poupin, N. Truffaut, B. Combourieu, P. Besse, M. Sancelme, H. Veschambre, A.M. Delort, Appl. Environ. Microbiol. 64 (1998) 159–165.
- [12] F.M. Bento, I.B. Beech, C.C. Gaylarde, G.E. Englert, I.L. Muller, Degredation and corrosive activities of fungi in a diesel–mild steel–aqueous system World Journal of Microbiology, Biotechnology 21 (2005) 135–142.
- [13] N. Muthukumar, S. Mohanan, S. Maruthamuthu, P. Subramanian, N. Palaniswamy, M. Raghavan, Role of *Brucella* sp. and *Gallionella* sp. in oil degradation and corrosion, Electrochem. Commun. 5 (2003) 421–427.
- [14] J.R. Romero Dominguez, G. Garcia Caloca, J. Mendoza Flores, E.M. Ibarra Nunez, Study on the presence of *Pseudomonas fluorescens* on the efficacy of three corrosion inhibitors (in Spanish), 3rd NACE Latin American Region Corrosion Congress, Cancun, Q. Roo, Mexico, Book of abstracts, pp. 51–52, (1998).
- [15] S. Maruthamuthu, S. Mohanan, A. Rajasekar, N. Muthukumar, S. Ponmarippan, P. Subramanian, N. Palaniswamy, Role of corrosion inhibitor on bacterial corrosion in petroleum product pipelines, Ind. J. Chem. Tech. 12 (5) (2005) 567–575.
- [16] S. Papavinasam, R.W. Review, M. Attard, A. Demoz, H. Sun, J.C. Donini, K.H. Michaelian, Laboratory methodologies for corrosion inhibitor selection, Mater. Perform. 39 (8) (2000) 58.
- [17] R.S. Treseder, R. Baboian, C.G. Munger, NACE Corrosion Engineer's Reference Book, NACE International, Houston, Texas, TIC 245834, 1991.
- [18] E. Rodriguez de Schiapparelli, B.R. de Meybaum, Microbial contamination and corrosion of aircraft integral fuel storage tanks—evaluation and risk control, Mater. Perform. 19 (10) (1980) 47.
- [19] E.R. Freiter, Effect of a corrosion inhibitor on bacteria and microbially influenced corrosion, Corrosion 48 (4) (1992) 266–276.
- [20] R. Prasad, Selection of Corrosion Inhibitors to Control Microbiologically Influenced Corrosion, CORROSION/98, Paper No. 276, NACE International, Houston, TX, 1998.